

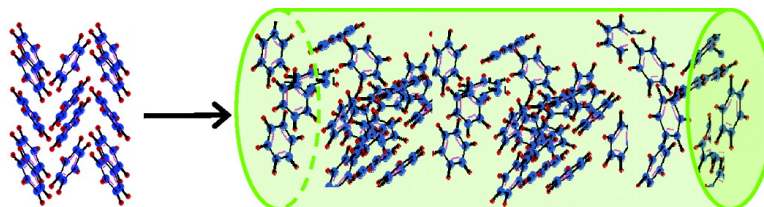
Article

A C NMR Study of the Molecular Dynamics and Phase Transition of Confined Benzene inside Titanate Nanotubes

Xiao-Ping Tang, Jing-Chen Wang, Lewis W. Cary, Alfred Kleinhammes, and Yue Wu

J. Am. Chem. Soc., **2005**, 127 (25), 9255-9259 • DOI: 10.1021/ja051628i • Publication Date (Web): 04 June 2005

Downloaded from <http://pubs.acs.org> on March 25, 2009



More About This Article

Additional resources and features associated with this article are available within the HTML version:

- Supporting Information
- Links to the 3 articles that cite this article, as of the time of this article download
- Access to high resolution figures
- Links to articles and content related to this article
- Copyright permission to reproduce figures and/or text from this article

[View the Full Text HTML](#)

A ^{13}C NMR Study of the Molecular Dynamics and Phase Transition of Confined Benzene inside Titanate Nanotubes

Xiao-Ping Tang,^{*,†} Jing-Chen Wang,[†] Lewis W. Cary,[‡] Alfred Kleinhammes,[§] and Yue Wu[§]

Contribution from the Departments of Physics and Chemistry, University of Nevada, Reno, Nevada 89557, and Department of Physics and Astronomy, University of North Carolina, Chapel Hill, North Carolina 27510

Received March 14, 2005; E-mail: x.p.tang@louisville.edu

Abstract: This work investigated the nanoconfinement effect on the molecular dynamics and phase transition of confined benzene inside titanate nanotubes with a uniform inner diameter of ~ 5.3 nm. For ^{13}C -enriched organics, the ^{13}C nuclear spin–spin relaxation was demonstrated as a sensitive tool to differentiate molecular translational motion and reorientation and, thus, was shown to be advantageous over the commonly employed ^1H and ^2H NMR for studying complex phase diagram, specifically, for separating the phase behavior of translational motion and the phase behavior of molecular reorientation. In such an approach, the melting of translational motion of confined benzene was explicitly observed to take place in a broad temperature range below the bulk melting temperature. The abrupt change of the ^{13}C nuclear spin–spin relaxation time of the confined liquid benzene at about 260 K suggested that nanoconfinement induced two topologically distinct liquid phases.

Introduction

Confined liquids are ubiquitous in nature. The enormous interest in this intriguing state stems from the fact that nanoconfinement can markedly change molecular structure,¹ molecular dynamics,^{1,2} and phase behavior.² Given the simple and uniform hollow cylindrical geometry, a nanotube provides an epitome host for studying liquid confinement. Nanotubes can be used to mimic biological nanotubular structures, and a comprehensive understanding of nanotube-confined liquids will lay a necessary foundation toward developing nanotube-based nanofluidic devices and nanochemistry. Over the past several years, a surging number of theoretical studies have been reported on this subject. For instance, a spectrum of novel dynamic and phase properties has been predicted for confined water in nanotubes.^{3–7} On the other hand, experimental studies were scanty. The employed techniques included TEM,⁸ SEM,⁹ neutron scattering,¹⁰ optical microscopy,¹¹ and nuclear magnetic

resonance (NMR).¹² NMR is routinely used to noninvasively study molecular dynamics and phase transition under demanding physical conditions, such as a wide temperature range. It has also been used for characterizing nanotubes.^{13,14} This work employed NMR to investigate the nanoconfinement effect on the molecular dynamics and phase transition of benzene confined inside titanate nanotubes.

In the liquid state, benzene molecules undergo rapid molecular translational motion and rapid molecular reorientation. Molecular reorientation of benzene includes two different modes: the isotropic reorientation of the 6-fold axis of the aromatic ring and the in-plane rotation around the 6-fold axis. Since the energy barrier for the former is larger than that of the latter, one expects that normally isotropic reorientation should freeze when in-plane rotation freezes. The reverse may not be true. Bulk benzene crystallizes at 278.49 K into an orthorhombic-like structure with the lattice constants as^{15,16} $a = 7.46$ Å, $b = 9.67$ Å, $c = 7.03$ Å, but de facto belonging to the crystallographic space group of *Pbca*. Crystallization freezes both translational motion and isotropic reorientation. However, the discrete rotational hopping around the fixed 6-fold axes remains active down to below 100 K.^{17,18} For confined benzene in clathrate,¹⁸

* Future mailing address: Xiaoping Tang, Department of Physics, University of Louisville, Louisville, KY 40292. Phone: (502) 852-6790. Fax: (502) 852-0742.

[†] Department of Physics, University of Nevada.

[‡] Department of Chemistry, University of Nevada.

[§] University of North Carolina.

- (1) Modig, K.; Liepinsh, E.; Otting, G.; Halle, B. *J. Am. Chem. Soc.* **2004**, *126*, 102–114.
- (2) Drake, J. M.; Klafter, J. *Phys. Today* **1990**, *43*, 46–55.
- (3) Hummer, G.; Rasaiah, J. C.; Noworyta, J. P. *Nature* **2001**, *414*, 188.
- (4) Koga, K.; Gao, G. T.; Tanaka, H.; Zeng, X. C. *Nature* **2001**, *412*, 802.
- (5) Berezhkovskii A.; Hummer, G. *Phys. Rev. Lett.* **2002**, *89*, 064503.
- (6) Mashl, R. J.; Joseph, S.; Aluru, N. R.; Jakobsson, E. *Nano Lett.* **2003**, *3*, 589.
- (7) Mann, D. J.; Halls, D. *Phys. Rev. Lett.* **2003**, *90*, 195503.
- (8) Gogotsi, Y.; Libera, J. A.; Yazicioglu, A. G.; Megaridis, C. M. *Appl. Phys. Lett.* **2001**, *79*, 1021.
- (9) Rossi, M. P.; Ye, H. H.; Gogotsi, Y.; Babu, S.; Ndungu, P.; Bradley, J.-C. *Nano Lett.* **2004**, *4*, 989.

- (10) Kolesnikov, A. I.; Zanotti, J.-M.; Loong, C.-K.; Thiyagarajan, P.; Moravsky, A. P.; Loutfy, R. O.; Burnham, C. J. *Phys. Rev. Lett.* **2004**, *93*, 035503.
- (11) Kim, B. M.; Sinha, S.; Bau, H. H. *Nano Lett.* **2004**, *4*, 2203–2208.
- (12) Tang, X.-P.; Chartkunchand, K. C.; Wu, Y. *Chem. Phys. Lett.* **2004**, *399*, 456–460.
- (13) Tang, X.-P.; Kleinhammes, A.; Shimoda, H.; Fleming, L.; Bonnoune, K. Y.; Bower, C.; Zhou, O.; Wu, Y. *Science* **2000**, *288*, 492–494.
- (14) Bac, C. G.; Bernier, P.; Latil, S.; Jourdain, V.; Rubio, A.; Jhang, S. H.; Lee, S. W.; Park, Y. W.; Holzinger, M.; Hirsch, A. *Curr. Appl. Phys.* **2001**, *1*, 149–155.
- (15) Cox, E. G.; Smith, J. A. *Nature* **1954**, *173*, 75.
- (16) Cox, E. G. *Rev. Mod. Phys.* **1958**, *30*, 159.

polymer matrix,¹⁹ mesoporous silica glasses, such as SBA-15^{20,21} and MCM-41,²¹ and controlled pore glasses,^{21,22} isotropic reorientation was observed to be active when translational motion was already frozen.^{20,21} The freezing of translational motion and isotropic reorientation took place typically in a broad temperature range and below the bulk freezing temperature.^{20,21} As a result, a complex dynamic phase diagram emerges from such systems rendering the Gibbs–Thomson equation inadequate, although it is commonly used to describe the depression of the melting temperature of confined liquids. In those studies, both isotropic reorientation and in-plane rotation of benzene molecules were quantified using the elaborate ²H quadrupolar-echo-line-shape analysis,^{18–20} exploiting the property that the quadrupolar interaction of the ²H spins is primarily determined by the relative orientation of the chemical bonds of benzene with respect to the applied external magnetic field. On the other hand, this method is insensitive to translational motion, an intermolecular motion. The thermal evolution of translational motion was monitored macroscopically by differential scanning calorimetry^{20,21} and microscopically by ¹H NMR.^{21,22}

This article explores the ¹³C NMR, particularly the ¹³C spin–spin relaxation, as a sensitive probe to separate molecular translational motion and reorientation for organic liquids and solids. In the current study, benzene was fully enriched with the ¹³C isotope, hence, denoted as ¹³C₆H₆. Thus, the characteristic ¹³C spin–spin relaxation time (T_2) is dominated by the homonuclear dipolar coupling (HDC) between the ¹³C nuclear spins.^{23,24} The second moment of HDC is often used to quantify T_2 .^{23,24} Since the dipolar coupling between two nuclear spins is inversely proportionate to the third power of the internuclear distance, the short C–C distance ($\approx 1.40 \text{ \AA}$)¹⁶ between the nearest neighbors of carbon nuclei within the aromatic ring derives a strong intramolecular ¹³C HDC. For fully frozen polycrystalline ¹³C₆H₆, the calculated second moment is $\langle \Delta\nu^2 \rangle_{\text{intra}} \approx 7.2 \times 10^6 \text{ Hz}^2$. With respect to the large $\langle \Delta\nu^2 \rangle_{\text{intra}}$, the ¹³C T_2 should become short when molecular reorientation of all modes is fully frozen. Even in a situation where in-plane rotation is fast but isotropic reorientation is frozen, the intramolecular HDC is only partially averaged out by the former.^{17,24} For a powder sample, the effective second moment is reduced^{17,24} to $\langle \Delta\nu^2 \rangle_{\text{intra}}/4$, thus doubly lengthening the ¹³C T_2 . Conversely, because the C–C distances between carbon nuclei residing in different benzene molecules are several times larger, the intermolecular ¹³C HDC is small. For a powder sample with the lattice structure similar to that of the orthorhombic-like bulk crystalline structure, the calculated second moment of the intermolecular HDC is only about $\langle \Delta\nu^2 \rangle_{\text{inter}} \approx 1.5 \times 10^5 \text{ Hz}^2$. Now, considering a benzene phase with frozen translational motion but fast isotropic reorientation, the inter-

molecular HDC alone is effective, whereby isotropic reorientation averages out the intramolecular HDC. In such a phase, the ¹³C T_2 is lengthened further by several times. Of course, one manifestation of the translationally mobile liquid is a typically very long T_2 , as a result of the fast molecular translational motion which averages out even the intermolecular HDC. Therefore, the ¹³C spin–spin relaxation measurement can identify various molecular dynamic states of benzene: (i) liquid; (ii) molecular translational motion is frozen, but molecular reorientation is active; (iii) molecular isotropic reorientation is frozen, while molecular in-plane rotation is active; and (iv) molecular in-plane rotation is also frozen. Note that both (i) and (ii) were taken as liquids in those studies employing the ²H quadrupolar-echo-line-shape analysis.²⁰ The focus of this report was to use the ¹³C NMR to explicitly resolve the states (i) and (ii) for the confined ¹³C₆H₆ in titanate nanotubes. It is hoped that the ¹³C nuclear spin–spin relaxation will be developed as a generalized tool to separate the molecular dynamic states for organics encountering complex phase diagrams. Inspecting the molecular structures, the intramolecular C–C distance is generally shorter than the intermolecular C–C distance. Therefore, in using ¹³C-enriched samples, the ¹³C spin–spin relaxation provides a sensitive tool to differentiate molecular translational motion and reorientational motion. By contrast, hydrogen atoms are not directly bonded with each other within the molecule and usually reside at the edge of the molecule. The distinction is thus much less between the intramolecular H–H distance and the intermolecular H–H distance. As such, the ¹H or ²H spin–spin relaxation is less sensitive for differentiating translational motion (intermolecular) and molecular reorientation (intramolecular), as evidently shown in the previous studies.^{21,22}

Materials and Methods

The titanate nanotubes were produced by the method of hydrothermal synthesis as described in the references.^{25–27} Specifically, the TiO₂ anatase microcrystals (from Aldrich with the average particle size of 32 nm and the specific surface area of 45 m²/g) were dissolved in 10 M NaOH solution and heated in a Teflon-lined autoclave at 130 °C for over 72 h. The resulting white precipitate, upon sonication, filtration, and repeated wash with distilled water, transformed into nanotubes. The signature Raman and X-ray spectra were used to confirm that the sample contains exclusively titanate nanotubes. The tube dimension and geometry were determined using transmission electron microscopy (TEM). Unlike single-walled carbon nanotubes, the titanate nanotubes are uncapped with a hollow semi-cylindrical center surrounding by a tube wall which resembles a scroll. The cross-sectional dimensions of titanate nanotubes are nearly uniform with inner and outer diameter, respectively, at about 5.3 and 12 nm. The interlayer distance of the wall is $\sim 0.7 \text{ nm}$. The tube length ranges from 0.3 to 1 μm . Thus, the aspect ratio between the tube length and the inner diameter is large.

A 5 mm diameter Wilmad NMR tube was loaded with 49 mg of titanate nanotubes and then filled with 114.1 mg of liquid benzene of ¹³C₆H₆ (99% ¹³C-enriched by Cambridge Isotope). The sample was sealed and then sonicated for 1 h. Before the NMR measurements, the mixture was set for 2 days. A layer of bulk phase of benzene was formed on the top and a paste-like mixture at the bottom. The ¹³C NMR measurements were conducted at 125.79 MHz using a 500 MHz Varian

- (17) Andrew, E. R.; Eades, R. G. *Proc. R. Soc. London, A* **1953**, A218, 537–552.
(18) Ok, J. H.; Vold, R. R.; Vold, R. L. *J. Phys. Chem.* **1989**, 93, 7618–7624.
(19) Schulz, M.; van der Est, A.; Rössler, E.; Kossmehl, G.; Vieth, H.-M. *Macromolecules* **1991**, 24, 5040–5045.
(20) Gedat, E.; Schreiber, A.; Albrecht, J.; Emmler, Th.; Shenderovich, I.; Findenegg, G. H.; Limbach, H.-H.; Buntkowsky, G. *J. Phys. Chem. B* **2002**, 106, 1977–1984.
(21) Dosseh, G.; Xia, Y. D.; Alba-Simionesco, C. *J. Phys. Chem. B* **2003**, 107, 6445–6453.
(22) Aksnes, D. W.; Kimtys, L. *Solid State Nucl. Magn. Reson.* **2004**, 25, 146–152.
(23) Abragam, A. *Principles of Magnetic Magnetism*; Clarendon Press: Oxford, 1961.
(24) Slichter, C. P. *Principles of Magnetic Resonance*; Springer-Verlag: Berlin, 1990.

- (25) Kasuga, T.; Hiramatsu, M.; Hoson, A.; Sekino, T.; Niihara, K. *Adv. Mater.* **1999**, 11, 1307.
(26) Ma, R. Z.; Bando, Y.; Sasaki, T. *Chem. Phys. Lett.* **2003**, 380, 577.
(27) Zhang, S.; Peng, L.-M.; Chen, Q.; Du, G. H.; Dawson, G.; Zhou, W. Z. *Phys. Rev. Lett.* **2003**, 91, 256103.

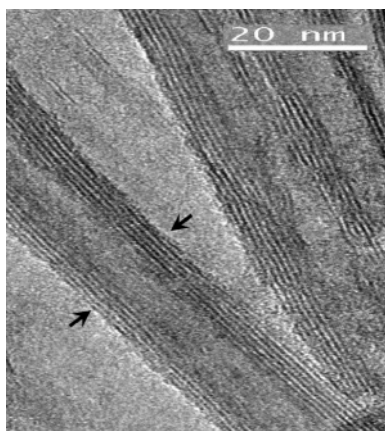


Figure 1. The TEM micrograph of titanate nanotubes showing a hollow semi-cylindrical center surrounded by the scroll-like tube wall. The two arrows point to the walls of the nanotube on the left (scale bar: 20 nm).

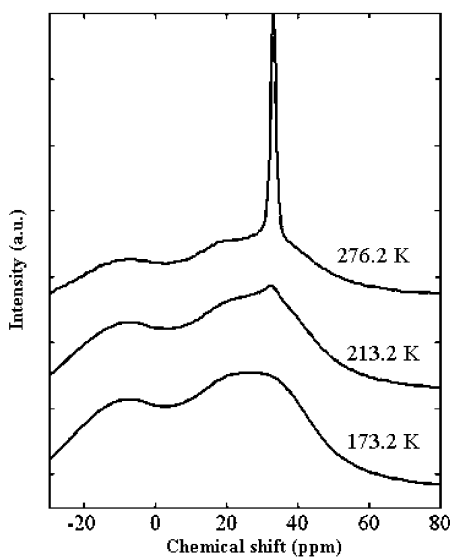


Figure 2. The ¹³C spectra (CDCl₃ as the reference for the chemical shift) measured at 276.2, 213.2, and 173.2 K by the spin-echo sequence with $2\tau = 40 \mu\text{s}$. For clarity of display, the spectra are shifted vertically from each other.

Unity^{plus} console and an 11.8 T OXFORD superconducting magnet. The calibrated 90° pulse for ¹³C nuclear spins was 5.8–6.0 μs and was determined at each temperature using the spin-echo pulse sequence “ $90^\circ - \tau - 180^\circ - \tau - \text{acquisition}$ ”. Using a Varian double resonance probe, the ¹³C NMR signal was acquired under proton decoupling. Considering that the ¹³C nuclear spin-lattice relaxation curve follows a stretched-exponential function form, the proper delay time between scans was chosen to ensure that at least 99% of the signal was recovered. Specifically, the delay time was 1.5 s at 173.2 K and was increased to 20 s at 276.2 K. The ¹³C NMR measurements were conducted between 298.2 and 173.2 K. The sample was initially cooled slowly to 173.2 K, at a cooling rate of about 5 K/1.5 min. The NMR measurement at 173.2 K was conducted 30 min after stabilizing the temperature. The sample was then slowly warmed to the desired temperatures. At each temperature, the NMR measurement was conducted 5–10 min after stabilizing the temperature. The temperature fluctuation was less than 0.3 K.

Results and Discussion

Figure 2 displays the ¹³C spectra measured at 276.2, 213.2, and 173.2 K by spin-echo with $2\tau = 40 \mu\text{s}$. Within the experimental error, the total intensity of the ¹³C spectra is

inversely proportionate to temperature, as expected by the Curie law. The broad line, with identical features at all of these temperatures, corresponds to the solid bulk benzene. The calculated nuclear spin dipolar coupling is too small to account for the large spectral width of the broad line. For the solid bulk benzene, the ¹³C NMR line is substantially broadened by the partially restored anisotropic chemical shift distribution²⁸ of benzene upon freezing isotropic reorientation and, to a lesser degree, upon freezing translational motion. It is remarkable that slowly cooling bulk benzene often produces several chunks of partially oriented benzene crystals.¹⁸ The resulted humped shape of the broad line can thus also serve as a signature for the bulk solid benzene. The measured ¹³C spin-spin relaxation time of the solid bulk benzene was $T_{2,\text{bulk}} \approx 88 \mu\text{s}$. The decrease of $T_{2,\text{bulk}}$ was measured to be less than 2% from 276.2 to 173.2 K. As discussed earlier, in this temperature range, $T_{2,\text{bulk}}$ should be dominated by the intramolecular ¹³C HDC, which is partially reduced by the fast in-plane rotation around the 6-fold axis.^{17,24} The tiny temperature dependence is likely originated from the small contraction of the bulk solid benzene upon cooling.¹⁵

In Figure 2, a narrow feature at about 33 ppm (here, CDCl₃ was used as reference) appears noticeably at 213.2 K and rather prominently at 276.2 K. Such a narrow feature has not been previously reported for the solid bulk benzene.²⁸ To identify the narrow feature, Figure 3a–b displays the ¹³C spectra acquired by spin-echo with different τ values. At 173.2 K (Figure 3a), for $2\tau \geq 700 \mu\text{s}$, the broad line of the bulk solid benzene becomes invisible because of the rapid decay with short $T_{2,\text{bulk}}$, whereas a much narrower and markedly different peak emerges at about 33 ppm. Thus, the narrow feature exists also at 173.2 K, and that, for short τ , is merely eclipsed by the dominating broad line of the bulk solid benzene. For the convenience of the following discussion, the observed narrow peak at 173.2 K is denoted as feature A. The measured spin-spin relaxation time of feature A at 173.2 K is $T_{2,\text{A}}(173.2 \text{ K}) \approx 258 \mu\text{s}$, about three times longer than $T_{2,\text{bulk}}$. Thus, for the benzene phase associated with feature A, the intramolecular ¹³C HDC is significantly smaller than that of the bulk solid benzene. It requires this benzene phase to retain active isotropic reorientation at 173.2 K, opposed to the bulk solid benzene. This is further confirmed by the much smaller line width of the corresponding peak. As discussed earlier, when isotropic reorientation is frozen, the spectrum should be markedly broadened by the partially restored anisotropic chemical shift distribution. Figure 3c displays the ¹³C spectra at 276.2 K with different τ values. Again, the broad peak of the bulk solid benzene vanishes at long τ , leaving behind a narrow peak. The narrow peak at 276.2 K, much narrower than feature A, is denoted as feature B. For feature B, the measured second moment calculated safely within 10 kHz from the peak position, which must contain the broadening by field inhomogeneity, etc., is only about 1/4 of the calculated $\langle \Delta\nu^2 \rangle_{\text{inter}}$. Therefore, in addition to rapid isotropic reorientation, this phase must also retain active translational motion to suppress at least partially the intermolecular ¹³C HDC. Moreover, the measured ¹³C spin-spin relaxation time of feature B is $T_{2,\text{B}}(276.2 \text{ K}) \approx 5.7 \text{ ms}$. The manifestly long $T_{2,\text{B}}$ and the narrow line width unquestionably identify feature B as a liquidlike benzene phase, retaining

(28) Pines, A.; Gibby, M. G.; Waugh, J. S. *Chem. Phys. Lett.* **1972**, *15*, 373–376.

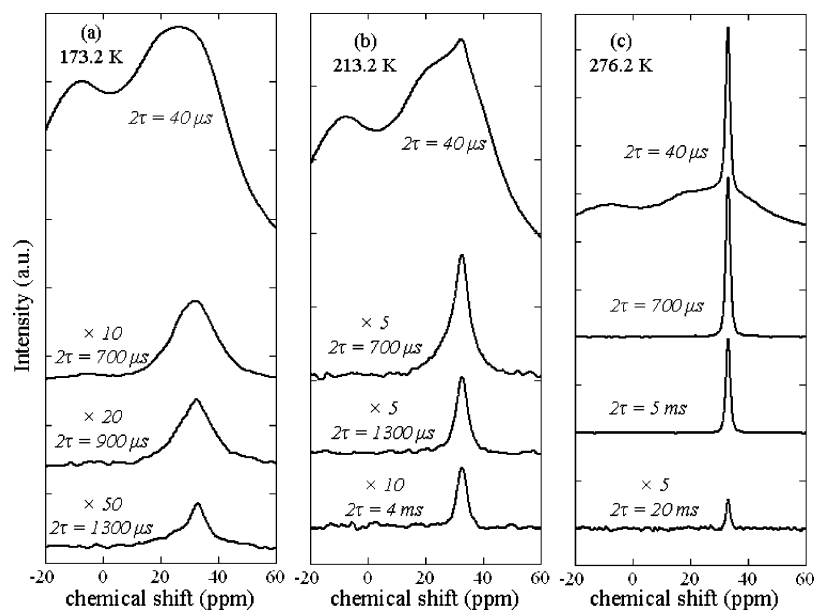


Figure 3. The ^{13}C spectra (CDCl_3 as the reference) measured by spin-echo: (a) at 173.2 K with $2\tau = 40, 700, 900,$ and $1300 \mu\text{s}$; (b) at 213.2 K with $2\tau = 40, 700, 1300,$ and $4000 \mu\text{s}$; (c) at 276.2 K with $2\tau = 40, 700, 5000,$ and $20\,000 \mu\text{s}$. For clarity of display, the spectra are shifted vertically from each other and some are magnified in amplitude by a factor indicated by the “ \times ” sign.

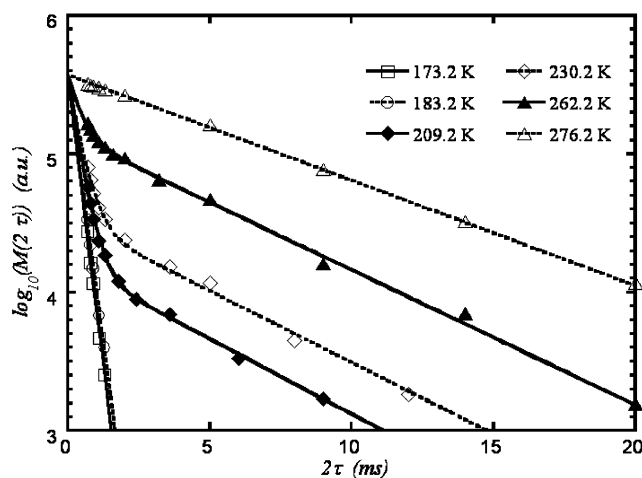


Figure 4. The ^{13}C nuclear spin-spin relaxation curves of confined benzene. The displayed nuclear spin magnetization $M(2\tau)$ is normalized by multiplying by the 173.2 K/T factor. The curve fittings are performed for the decay time of $2\tau \geq 700 \mu\text{s}$.

both fast isotropic reorientation and translational motion. Figure 3b displays the ^{13}C spectra acquired at 213.2 K. The narrow feature at $2\tau = 700 \mu\text{s}$ comprises two overlapping peaks. The broader peak decays faster as τ increases with the corresponding $T_2 \approx 336 \mu\text{s}$. Thus, it resembles feature A. With a markedly longer $T_2 \approx 4.1 \text{ ms}$, the narrower peak resembles feature B. The salient feature of Figure 3 is examined further in Figure 4.

Figure 4 displays the ^{13}C nuclear spin-spin relaxation curves between 276.2–173.2 K, depicting the measured nuclear spin magnetization of $M(2\tau)$ by spin-echo as a function of 2τ . To account for the Curie law, the displayed $M(2\tau)$ is normalized at 173.2 K by multiplying the measured spectral intensity by the $173.2/T$ factor (T as the observation temperature). Since the broad line of the bulk solid benzene becomes negligible for $2\tau \geq 700 \mu\text{s}$ (Figure 3), the analysis of the $M(2\tau)$ curve is performed for $2\tau \geq 700 \mu\text{s}$, such that $M(2\tau)$ contains only feature A and feature B. As shown, at 173.2 and 183.2 K, $M(2\tau)$

can be described by a fast-decaying component of $T_{2,A}$. At 276.2 K, $M(2\tau)$ is described by a slow-decaying component of $T_{2,B}$. Their prefactors, by extrapolating $M(2\tau)$ to $2\tau = 0$, are, however, about the same. It indicates that feature A and feature B originate from the same part of the benzene sample. Upon heating from 173.2 to 276.2 K, this part of the sample evolves from a translationally immobile phase (feature A) to a liquid phase (feature B), although both retain isotropic reorientation. This part of the benzene sample, differing from the bulk solid benzene, is ascribed to the confined benzene inside the titanate nanotubes. For the intermediate temperature range in Figure 4, the $M(2\tau)$ curves comprise a slow-decaying component resembling feature B and a fast-decaying component resembling feature A. Thereby, the spectral shape analysis (Figure 3) and the spin-spin relaxation analysis (Figure 4) both infer that in the intermediate temperature range, two benzene phases coexist in the confined benzene; one retains active isotropic reorientation but is frozen in translational motion; the other is a liquid undergoing fast molecular translational motion and reorientation. Therefore, advantageous over the ^2H quadrupolar-echo-line-shape analysis in this respect, the current ^{13}C spin-spin relaxation analysis indeed clearly resolved these two phases.

To quantitatively examine the phase transition upon heating, the $T_{2,A}(T)$ of feature A and the $T_{2,B}(T)$ of feature B are displayed in Figure 5a, obtained by fitting the ^{13}C spin-spin relaxation curves as shown in Figure 4. The respective prefactors $M_A(T)$ and $M_B(T)$ are displayed in Figure 5b. As shown, the sum, $M_A(T) + M_B(T)$, is approximately constant in the entire temperature range of the current study. The ^2H quadrupolar-echo-line-shape analysis often observes^{18,29} a decrease of the intensity induced by the exchange broadening when reorientation reaches the intermediate frequency. However, in the temperature range of the current study, translational motion, fast or slow, does not induce significant change of the chemical shift; indeed, for the current study, the active molecular reorientation averages out the chemical shield tensor. The $M_B(T)$ curve shows that a

(29) Speiss, H. W.; Sillescu, H. *J. Magn. Reson.* **1981**, *42*, 381–389.

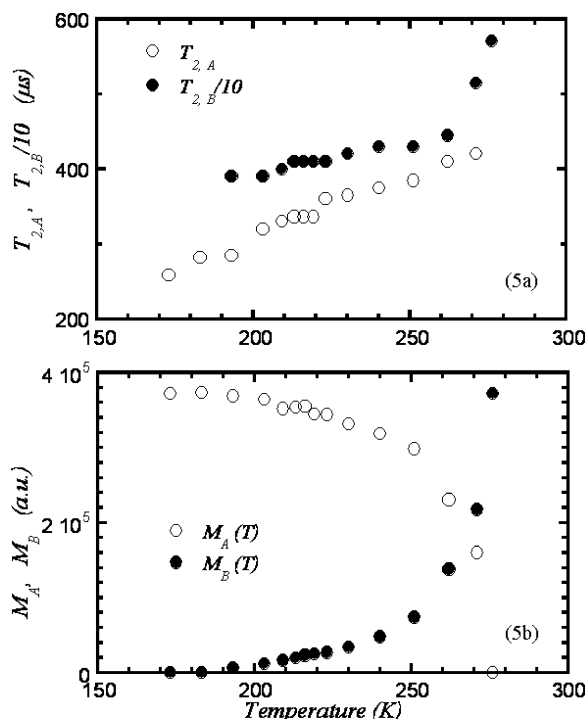


Figure 5. (a) $T_{2,B}(T)/10$ as a function of temperature for the confined liquid benzene corresponding to feature B, and $T_{2,A}(T)$ for the confined solid benzene corresponding to feature A. (b) The respective prefactors, $M_A(T)$ and $M_B(T)$ of features A and B versus the temperature.

small portion of the confined benzene becomes translationally mobile even at 193.2 K, well below the bulk melting temperature (278.2 K). However, the percentage of the liquid phase over the total confined benzene increases only gradually as T increases; the liquid phase reaches 1/3 at about 260 K. Melting takes place primarily above 260 K. Notably, $T_{2,B}(T)$ decreases rapidly from 276 to 260 K, but remains approximately constant below 260 K. In the entire temperature range, $T_{2,B}(T)$ is more than 10 times longer than $T_{2,A}(T)$. The monotonic decrease of $T_{2,A}(T)$ as T decreases should reflect the gradual decrease of isotropic reorientation. However, at high temperatures, it may contribute, in part, to gradual freezing of any residual translational motion or in-cage collision if assuming a loose local structure under confinement. Then, it becomes complicated for quantitative extraction of the decrease of isotropic reorientation from the present $T_{2,A}(T)$ curve. In the future, the $T_{2,A}(T)$ curve will be acquired in the lower temperature range to examine the freezing of isotropic reorientation.

Regarding confined liquids inside small pores, it has been speculated^{2,20,21} that one to two surface layers of the confined liquid melt at temperatures lower than that of the central layers away from the pore walls. Although complex mechanisms were proposed^{20,21} to account for the bigger depression of the melting temperature of the surface layers, the putative mechanisms are yet to be corroborated. Nevertheless, the current results displayed in Figure 5 are in accord with such a scenario. Assuming the local structure of confined benzene is similar to the innate structure of bulk benzene, the distance between the nearest benzene molecules is about 5 Å. Given the 5.3 nm inner diameter of titanate nanotubes, a nanotube can accommodate roughly a little more than five layers of benzene molecules.

For such a structure, the surface layer, directly interacting with the tube wall and under the topological constrain, constitutes approximately 1/2–1/3 of the total confined benzene. Assuming that melting of the surface layer is further depressed compared to the center layers, Figure 5 indeed shows that about 1/3 of the confined benzene melts at lower temperature, below 260 K. In view of this, they are assigned to the surface layer. Thus, the surface layer melts below 260 K in a broad temperature range, while the melting of the center layers takes place above 260 K. It is likely that the center layers retain a more homogeneous environment and retain a structure closer to that of the innate bulk benzene phase. This may explain that melting of the center layers takes place in a narrower temperature range. The noticeable kink of the $T_{2,B}(T)$ curve at 260 K (Figure 5a) may correlate with the change from the surface-layered liquid phase to the multilayered liquid phase. When the surface layer alone is melted, molecular translational motion should be topologically restricted to a loose 2D cylindrical layer. Since such quasi-2D translational motion is less effective to average out the intramolecular ¹³C HDC than the 3D translational motion in bulk liquids, $T_{2,B}$ should be shorter below 260 K, as shown in Figure 5a. Further, two features are of interest: the long tail of the melting temperature of the surface layer, and within this broad temperature range, $T_{2,B}$ remains long and approximately constant. These features evoke a heterogeneous mechanism of the melting of the surface layer. Heterogeneity can arise from the nonuniformity among nanopores or the nonuniformity within each pore, or it simply reveals the much-sought intrinsic nature of glassy systems. The first origin for heterogeneity may be ruled out in this study given the generally excellent uniformity among nanotubes such as titanate nanotubes. Nevertheless, a definitive conclusion on this important issue invites future studies.

Conclusions

In summary, ¹³C NMR was employed to study the molecular dynamics and phase transition of confined benzene inside titanate nanotubes. The ¹³C nuclear spin–spin relaxation was demonstrated as a sensitive tool to differentiate molecular translational and reorientational dynamics for ¹³C-enriched organics. The melting of the translational motion of the confined benzene was explicitly observed to take place in a broad temperature range below the bulk melting point. An abrupt change was observed at about 260 K for the ¹³C spin–spin relaxation behavior of the confined benzene liquid. It suggested the thermal evolution through two topologically distinct liquid phases: (i) at low temperature, only the surface layer of the confined benzene, in direct contact with the tube wall, remains translationally mobile; (ii) at high temperature, the confined benzene inside a nanotube is entirely translationally mobile.

Acknowledgment. This work was supported by NSF under Contract DMR-0139452, and by ARO under Contract DAAD19-03-1-0326. This work was supported in part by a grant from the University of Nevada, Reno, Junior Faculty Research Grant Fund. This support does not necessarily imply endorsement by the university of research conclusions.

JA051628I